Minor Groove Binding DNA Ligands with Expanded A/T Sequence Length Recognition, Selective Binding to Bent DNA Regions and Enhanced Fluorescent Properties†

Urmila Tawar,‡ Akash K. Jain,‡ Ramesh Chandra,‡ Yogendra Singh,‡,⊥ B. S. Dwarakanath,§ N. K. Chaudhury,§ Liam Good,|| and Vibha Tandon*,‡

Dr. B. R. Ambedkar Center for Biomedical Research, University of Delhi, Delhi-110007, India, Institute of Genomics and Integrative Biology, Mall Road, Delhi-110007, India, Institute of Nuclear Medicine and Allied Sciences, Brig. S. K. Majumdar Road, Delhi-110054, India, and Center for Genomics and Bioinformatics, Karolinska Institutet 17177 Stockholm, Sweden

Received March 17, 2003; Revised Manuscript Received August 26, 2003

ABSTRACT: DNA minor groove ligands provide a paradigm for double-stranded DNA recognition, where common structural motifs provide a crescent shape that matches the helix turn. Since minor groove ligands are useful in medicine, new ligands with improved binding properties based on the structural information about DNA−ligand complexes could be useful in developing new drugs. Here, two new synthetic analogues of AT specific Hoechst 33258 5-(4-methylpiperazin-1-yl)-2-[2′-(3,4-dimethoxyphenyl)-5′-benzimidazolyl] benzimidazole (DMA) and 5-(4-methylpiperazin-1-yl)-2-[2′{2″-(4-hydroxy-3-methoxyphenyl)-5″-benzimidazolyl}-5′-benzimidazolyl] benzimidazole (TBZ) were evaluated for their DNA binding properties. Both analogues are bisubstituted on the phenyl ring. DMA contains two ortho positioned methoxy groups, and TBZ contains a phenolic group at C-4 and a methoxy group at C-3. Fluorescence yield upon DNA binding increased 100-fold for TBZ and 16-fold for DMA. Like the parent compound, the new ligands showed low affinity to GC-rich ($K \approx 4 \times 10^7$ M^{-1}) relative to AT-rich sequences ($K \approx 5 \times 10^8$ M^{-1}), and fluorescence lifetime and anisotropy studies suggest two distinct DNA−ligand complexes. Binding studies indicate expanded sequence recognition for TBZ (8−10 AT base pairs) and tighter binding (ΔT_m of 23 °C for d (GA_5T_5C). Finally, EMSA and equilibrium binding titration studies indicate that TBZ preferentially binds highly hydrated duplex domains with altered A-tract conformations d $(GA_4T_4C)_2$ ($K = 3.55 \times 10^9$ M^{-1}) and alters its structure over d $(GT_4A_4C)_2$ ($K = 3.3 \times 10^8$ M^{-1}) sequences. Altered DNA structure and higher fluorescence output for the bound fluorophore are consistent with adaptive binding and a constrained final complex. Therefore, the new ligands provide increased sequence and structure selective recognition and enhanced fluorescence upon minor groove binding, features that can be useful for further development as probes for chromatin structure stability.

Drugs that bind within the DNA minor groove are of considerable interest for their antimicrobial and antitumor activities and applications in biological research as reagents to probe DNA structures. Antibiotics distamycin and netropsin as well as fluorochromes such as 4′,6-diamidino-2-phenylindole (DAPI) and 2-(4-hydroxyphenyl)-5-(4-methyl-1-piperazinyl)-2,5′-bi-1*H*-benzimidazole (Hoechst 33258) are among the well-known examples of minor groove binding agents. Further, DAPI and Hoechst 33258 very well-suited to study the mechanisms of action of several drugs on cells because of their fluorescence characteristics (*1*, *2*). Unfortunately, wider use in medicine and research is limited by nonspecific inhibition of gene expression and high general toxicity (*3*).

All minor groove ligands possess common structural motifs that allow them to adopt a crescent shape that matches the turn of the DNA double helix (*4*). Results from footprinting studies of Hoechst 33258 with methidiumpropyl EDTA-Fe (II) show that it covers three to five base pairs involving predominantly AT bases (*5*), which has been supported by studies using ^{125}I -labeled Hoechst that cleaves double-stranded DNA (*6*). Further, high-resolution crystallographic X-ray diffraction data have clearly shown that binding occurs within the minor groove interacting mainly with the central AT base pairs involving the N1 and N3 residues of the two benzimidazole rings (*7*). When bound to the polynucleotides poly [d $(I\text{-}C)_2$] and poly [d $(A\text{-}T)_2$], Hoechst exhibits an average orientation angle of near 45° relative to the DNA helix axis for the long axis polarized low-energy transition. By contrast, when bound to poly [d $(G\text{-}C)_2$] and poly [d $(G\text{-}m5C)_2$], Hoechst shows a distinctively different behavior. ^{1}H NMR studies of Hoechst complexed with d $(CTTTTGCAAAAG)_2$ in solution reveal that two drug molecules bind cooperatively within the minor groove in a symmetry-related orientation between the 5′-TTTT and the 5′-AAAA sequences (*8*). Therefore, ligand binding to dsDNA does not appear to be simple, although it clearly occurs within the minor groove and is influenced by base composition. Therefore, systematic studies by designing

† U.T. is thankful to the Council of Scientific and Industrial Research, India for financial assistance as a fellowship.

* Corresponding author.Telephone: 91-11-27666272 ext 248. Fax: 91-11-27666248. E-mail: vtandon@acbrdu.edu.

‡ Dr. B. R. Ambedkar Center for Biomedical Research.

§ Institute of Nuclear Medicine and Allied Sciences.

|| Karolinska Institutet.

⊥ Institute of Genomics and Integrative Biology.

10.1021/bi034425k CCC: $25.00
Published on Web 10/21/2003

analogues with improved sequence selectivity would facilitate a comprehensive understanding of ligand−DNA interaction leading to the development of better fluorescent probes and drugs.

In the present paper, we have evaluated DNA binding and sequence recognition properties of two synthetic analogues of Hoechst 33258, a bisbenzimidazole (DMA)[1] (*9*) as well as a trisbenzimidazole (TBZ) having bisubstitution on the phenyl ring, synthesized to increase the hydrogen bonding between the DNA and the ligand based on QSAR and molecular modeling (*10*). The two methoxy groups of DMA were chosen to increase the relative electron density at the two nitrogens of the imidazole ring in comparison to Hoechst 33342, whereas the TBZ has one methoxy and a hydroxy group ortho to each other on the phenyl ring (*11*). Interaction of these two analogues with DNA was analyzed by solution studies using UV, fluorescence spectroscopy, equilibrium binding titrations, and gel mobility shift assays. To understand the sequence recognition and specificity of these analogues, the binding studies were carried out with CTDNA and five synthetic oligonucleotides to restrict the binding site. The results show that the TBZ binds d (GA_5T_5C) with increased stability and has greater selectivity for d $(GA_4T_4C)_2$ over d $(GT_4A_4C)_2$ sequences. Structural changes or conformational restriction also appears to occur within the ligands as shown by increased fluorescence intensity upon binding. Furthermore, this study suggests that the TBZ alters the DNA structure in a manner that results in altered enzyme mediated DNA cleavage and can be used to probe DNA structure within chromosomes.

EXPERIMENTAL PROCEDURES

Chemicals. The compounds DMA and TBZ (Figure 1) were prepared by the published method (*11*). They were characterized by IR, NMR, and mass spectra analysis and were shown to be pure by HPLC.

Oligonucleotides. HPLC purified oligodeoxynucleotides were purchased from Technoconcept Microsynth, Switzerland. DNA duplexes were prepared from equimolar solutions of monomers in sodium cacodylate buffer (2 mM sodium cacodylate, 0.1 mM EDTA, 50 mM NaCl, 12 mM $MgCl_2$), heated to 94 °C for 3 min (*12*), and then cooled slowly to room temperature. The molar concentration was determined by absorbance measurements (Beer's law). The extinction coefficients of the duplexes were derived from a thermal denaturation curve, the ϵ_{260} values for the single strands being given by the supplier. CTDNA sodium salt was purchased from E-Merck, Germany.

Absorption Spectroscopy. DNA−drug interactions were monitored using spectroscopic techniques from changes in absorption and fluorescence spectra upon binding. A 10^{-6} M solution of DMA and TBZ was prepared in sodium cacodylate buffer (2 mM, pH = 7.2), and the absorbance spectra were recorded using a UV−vis spectrophotometer (GBC-916, Australia). Molar extinction coefficients were measured in deionized distilled water (pH = 7.2), and these were found to be $\epsilon_{340} = 20\,300$ for DMA and $\epsilon_{350} = 16\,600$ for TBZ. The absorbance of the new ligands was compared with Hoechst 33342 (10^{-6} M). The drug−DNA solutions were prepared in sodium cacodylate buffer (2 mM, pH = 7.2). DNA and drug mixtures were equilibrated for 25 min, and spectral measurements were recorded using a 1 cm path length quartz cell over 200−500 nm. For CTDNA, measurements were made at $R = 0.01$ and 0.1.

T_m Studies. T_m measurements were performed on a GBC 916 spectrophotometer and a Cary UV−vis spectrophotometer using 1 cm path length quartz cells equipped with a thermoprogrammer. Absorbance was monitored at 260 nm, while the temperature was raised from 25 to 100 °C at the rate of 0.5°/min with a stability of 0.2 °C. The transition melting temperature T_m was determined at the midpoint of the normalized curves.

Fluorescence Spectroscopy. The fluorescence and anisotropy data were obtained using a custom designed and integrated steady state and time-resolved spectrofluorimeter (FS900/FL900CDT, Edinburgh Analytical Instruments, UK). The solutions of DMA, TBZ, and Hoechst (10^{-6} M) were prepared in deionized water. The instrument parameters were as follows: $\lambda_{ex} = 340$ nm, slit = 10 mm, EHT = 6.7, gap = 0.8 mm, and frequency = 40 kHz. The data acquisition was based on a time-correlated single-photon counting (TCSPC) technique. The drug−DNA complexes were prepared in the sodium cacodylate buffer (2 mM, pH = 7.2) and incubated for 25 min to achieve maximum binding. Binding of DMA and TBZ with oligonucleotides was recorded at $R = 0.5$. The measurements were made using a 1 cm path length quartz cell ($\lambda_{ex} = 350$ nm). Anisotropy measurements and fluorescence lifetime decay profiles of the drug−DNA complexes ($R = 0.5$) were also recorded.

Equilibrium Binding Titrations. The binding constants of DMA and TBZ to DNA were obtained as described (*13*, *14*). Absorption titrations were carried out by keeping the concentration of ligand constant while adding a concentrated solution of the oligonucleotides in progressively increasing amounts into both cuvettes until saturation was observed. The intrinsic binding constant for the ligand with oligonucleotides was determined by the half-reciprocal plot method as described earlier (*15*−*18*). The intrinsic binding constant (K) for a given complex with oligonucleotide was obtained from a plot of $D/\Delta\epsilon_{ap}$ versus D according to the equation $D/\Delta\epsilon_{ap} = D/\Delta\epsilon + 1/(\Delta\epsilon K)$, where D is the concentration of DNA in base molarity and $\Delta\epsilon_{ap} = |\epsilon_a - \epsilon_f|$ and $\Delta\epsilon = |\epsilon_b - \epsilon_f|$, where ϵ_b and ϵ_f are respective extinction coefficients of the complex in the presence and absence of DNA. The apparent extinction coefficient, ϵ_a, was obtained by calculating A_{obsd}/[complex]. The data were fitted to the equation, with a slope equal to $1/\Delta\epsilon$ and y-intercept equal to $1/(\Delta\epsilon K)$. The intrinsic binding constant (K) was determined from the ratio of the slope to the y-intercept. The graphs were plotted using Graphpad Prism version 3.0.

Polyacrylamide Gel Electrophoresis (PAGE). Nondenaturing PAGE 25% (1 bisacrylamide/29 acrylamide) was conducted at room temperature. Both the gel and the running buffer contained 89 mM Trisborate (pH 8.0), 10 mM $MgCl_2$, and 2 mM Na_2EDTA. The ligand/DNA ratio was $R = 0.5$ with 100 μM duplex concentration. Glycerol was added [5% (vol/vol)], and a final sample volume of 18 μL was loaded

[1] Abbreviations: DMA, 5-(4-methylpiperazin-1-yl)-2-[2′-(3,4-dimethoxyphenyl)-5′-benzimidazolyl] benzimidazole; TBZ, 5-(4-methylpiperazin-1-yl)-2-[2′{2″-(4-hydroxy-3-methoxyphenyl)-5″-benzimidazolyl}-5′-benzimidazolyl] benzimidazole; CTDNA, calf thymus DNA; T_m, melting temperature; r, anisotropy; R_f, relative fluorescence enhancement; K, intrinsic binding constant; R, drug/DNA ratio.

Table 1: Physical Parameters for the Binding of Hoechst 33342, DMA, and TBZ to the CTDNA (100 μM) and d ($CGCA_3T_3GCG$), d (GA_5T_5C), d (GCATGGCCATGC), d $(GA_4T_4C)_2$, and d $(GT_4A_4C)_2$ Duplexes (5 μM) in 2 mM Sodium Cacodylate Buffer (pH = 7.2) Containing 50 mM NaCl, 0.1 mM EDTA, and 12 mM $MgCl_2$ at 25 °C[a]

study system	$\lambda_{ex/em}$	T_m (°C)	ΔT_m (°C)	aniso-tropy
CTDNA (100 μM)		70		
CTDNA + Hoechst 33342 ($R = 0.01$)	354/472	72	2	0.3
CTDNA + DMA ($R = 0.01$)	354/474	72.8	2.8	0.3
CTDNA + TBZ ($R = 0.01$)	355/460	70.2	0.2	0.3
CTDNA + Hoechst 33342 ($R = 0.1$)	354/484	78	8	0.3
CTDNA + DMA ($R = 0.1$)	354/484	76	6	0.3
CTDNA + TBZ ($R = 0.1$)	356/391, 418, 441	76.4	6.4	0.3
d ($CGCA_3T_3GCG$) (5 μM)		51		
d ($CGCA_3T_3GCG$) + Hoechst33342 ($R = 0.5$)	350/456, 485	40,67	16	0.28
d ($CGCA_3T_3GCG$) +DMA ($R = 0.5$)	350/456, 485	39,66	15	0.28
d ($CGCA_3T_3GCG$) + TBZ ($R = 0.5$)	358/395, 417, 442	39,72	21	0.3
d (GA_5T_5C) (5 μM)		39		
d (GA_5T_5C) + Hoechst 33342 ($R = 0.5$)	350/457, 480	49	10	0.22
d (GA_5T_5C) + DMA ($R = 0.5$)	350/457, 480	49	10	0.22
d (GA_5T_5C) + TBZ ($R = 0.5$)	360/395, 417, 443	62	23	0.31
d (GCATGGCCATGC) (5 μM)		50		
d (GCATGGCCATGC) + Hoechst 33342 ($R = 0.5$)	360/498	58	8	0.2
d (GCATGGCCATGC) + DMA ($R = 0.5$)	340/475	55	5	0.1
d (GCATGGCCATGC) + TBZ ($R = 0.5$)	365/505	55	5	0.2
d $(GA_4T_4C)_2$ (5 μM)		56		
d $(GA_4T_4C)_2$ + Hoechst 33342 ($R = 0.5$)	348/466	62	6	0.3
d $(GA_4T_4C)_2$ + DMA ($R = 0.5$)	348/468	65	9	0.3
d $(GA_4T_4C)_2$ + TBZ ($R = 0.5$)	348/395, 419, 441	57	1	0.3
d $(GT_4A_4C)_2$ (5 μM)		58		
d $(GT_4A_4C)_2$ + Hoechst 33342 ($R = 0.5$)	366/458	68	10	0.3
d $(GT_4A_4C)_2$ + DMA ($R = 0.5$)	348/458	72	14	0.3
d $(GT_4A_4C)_2$ + TBZ ($R = 0.5$)	368/491	60	2	0.3

[a] $\lambda_{ex/em}$ for Hoechst 33342 = 340/500 nm, DMA = 340/495 nm, and TBZ = 350/490 nm.

onto the gel and electrophoresed at 12 V/cm. The gels were stained using ethidium bromide, and images were captured using a BIO-RAD gel documentation system.

RESULTS

Absorbance Measurements. To assess the binding properties of DMA and TBZ in comparison to Hoechst 33342, the spectroscopic properties of free ligands and their complex with CTDNA and five duplex oligonucleotides were studied by absorbance spectroscopy (Table 1). TBZ showed no spectral shift upon binding with CTDNA at $R = 0.01$ and $R = 0.1$. Significant differences could not be observed in the binding behavior of Hoechst 33342, DMA, and TBZ with the duplex d (GCATGGCCATGC), which suggests that they bind in a noncooperative manner with no differential recognition of GC-rich DNA. To further understand the difference in the binding behavior between Hoechst 33342, DMA, and TBZ, their interactions with two more oligonucleotides d $(GA_4T_4C)_2$ and d $(GT_4A_4C)_2$ at a ligand/DNA

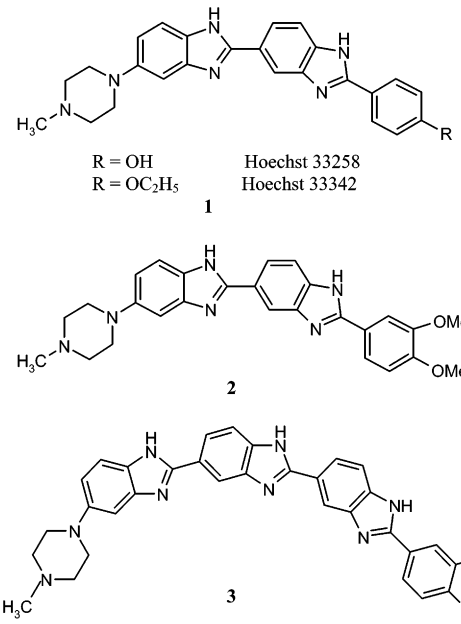

FIGURE 1: Chemical structures of the minor groove binding ligands: Hoechst 33258 **1**; Hoechst33342 **1**; DMA **2**, 5-(4-methylpiperazin-1-yl)-2-[2′-3,4-dimethoxyphenyl)-5′-benzimidazolyl] benzimidazole; and TBZ **3**, 5-(4-methylpiperazin-1-yl)-2-[2′{2″-(4-hydroxy-3-methoxyphenyl)-5″-benzimidazolyl}-5′-benzimidazolyl] benzimidazole.

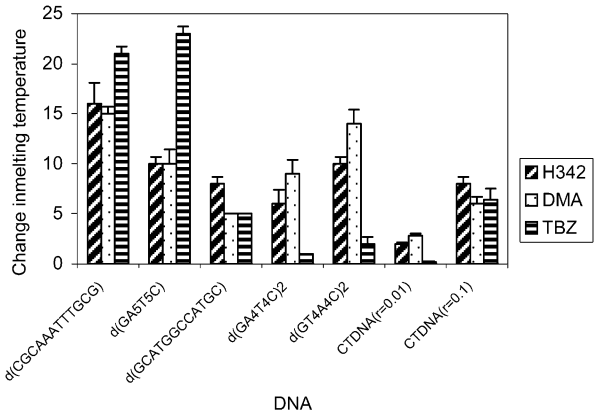

FIGURE 2: Graphical representation of ΔT_m of Hoechst 33342, DMA, and TBZ with CTDNA at $R = 0.1$ and d ($CGCA_3T_3GCG$), d (GA_5T_5C), d (GCATGGCCATGC), d $(GA_4T_4C)_2$, and d $(GT_4A_4C)_2$ duplexes at $R = 0.5$ in 2 mM sodium cacodylate buffer (pH = 7.2) containing 50 mM NaCl, 0.1 mM EDTA, and 12 mM $MgCl_2$ at 25 °C.

ratio ($R = 0.5$) were studied. While changes were not observed for Hoechst 33342, DMA, and TBZ upon binding to d $(GA_4T_4C)_2$, these ligands displayed a different behavior when bound to d $(GT_4A_4C)_2$. Hoechst 33342 showed a bathochromic shift of 26 nm, whereas DMA upon binding to DNA showed a bathochromic shift of only 8 nm. TBZ showed a bathochromic shift of 23 nm. Therefore, the results indicate nonspecific binding to these DNA duplexes.

Melting Temperature Measurements. To further assess the DNA binding properties of the ligands, the melting temperature for the DNA duplex in the presence and absence of ligand was determined, where the T_m increase can reflect ligand affinity assuming there is no enthalpy effect between the different ligands (Table 1, Figure 2). Thermal melting curves of Hoechst 33342, DMA, and TBZ showed a biphasic transition upon binding to d ($CGCA_3T_3GCG$). Hoechst 33342

and DMA showed a ΔT_m of 15 °C, while it was 21 °C with TBZ suggesting that TBZ stabilizes the duplex better than Hoechst 33342 or DMA. It also suggests that TBZ requires at least A_3T_3 for strong binding. Upon binding to the duplex d (GA_5T_5C), Hoechst 33342 and DMA showed a ΔT_m of 10 °C, whereas TBZ showed a ΔT_m of 23 °C. This very high ΔT_m upon the binding of TBZ to the longer sequence clearly implies that TBZ recognizes 10 base pairs rather than 6 base pairs as reported for other terbenzimidazoles (*19*). Interestingly, none of these ligands showed much difference in the melting temperature upon binding to d (GCATGGCCATGC). With d $(GA_4T_4C)_2$, Hoechst 33342 and DMA showed a ΔT_m of 6 and 9 °C, respectively, while TBZ had no significant effect on T_m. Similarly, d $(GT_4A_4C)_2$ upon binding to Hoechst 33342, DMA, and TBZ showed a ΔT_m of 10, 14, and 2 °C, respectively. Therefore, increased T_m for duplex DNA in the presence of new ligands is consistent with stable binding, particularly for the TBZ compound.

Emission Spectroscopy. Fluorescence emission of DNA binding ligands alone and of the complex indicate conformational changes or constraints that occur upon binding. TBZ showed three emission maxima with CTDNA, d ($CGCA_3T_3GCG$), d (GA_5T_5C), and d $(GA_4T_4C)_2$, whereas a single-emission maxima was observed with d (GCATGGCCATGC) and d $(GT_4A_4C)_2$. Further, TBZ showed a red shift of 15 nm with d (GCATGGCCATGC) and almost no shift with d $(GT_4A_4C)_2$ (Table 1). The fluorescence characteristics of Hoechst 33342 and DMA either alone or in their complex with duplex oligonucleotides including CTDNA were essentially similar (Table 1). There was a remarkable increase in the relative fluorescence (R_f) of DMA and TBZ upon binding to DNA as compared to Hoechst 33342 ($R_f = 1$). At $R = 0.01$ with CTDNA, DMA showed an R_f value of 12, whereas the R_f value for TBZ was 100. As the drug/DNA ratio is increased to $R = 0.05$, the fluorescence intensity of DMA modestly increased with $R_f = 16$, whereas TBZ showed a tremendous increase in fluorescence ($R_f = 200$). The anisotropy values for all the three ligands was essentially similar with CTDNA, d $(GA_4T_4C)_2$, and d $(GT_4A_4C)_2$ ($r = 0.3$); whereas with d ($CGGCA_3T_3GCG$), Hoechst 33342 and DMA showed $r = 0.28$, while TBZ showed a value of 0.30. With d (GA_5T_5C), Hoechst 33342 and DMA showed $r = 0.22$, whereas TBZ showed a value of 0.31. In case of d (GCATGGCCATGC), the anisotropy value with DMA was 0.1, while Hoechst 33342 and TBZ showed $r = 0.2$, which was significantly different than the other two ligand−DNA complexes (Table 1 and Figure 3). These observations clearly show that the binding of the new ligands to duplex DNA results in a remarkable increase in fluorescence intensity, consistent with structural alterations or constraints within the bound fluorophore.

Lifetime Measurements. To assess the level of heterogeneity for the DNA−ligand complexes, their fluorescence decay profiles were determined and used to calculate fluorescence lifetimes through deconvolution. In general, all three ligands have depicted two distinct fluorescence lifetimes (τ_1 and τ_2). Upon binding to CTDNA, d ($CGCA_3T_3GCG$), d (GA_5T_5C), d (GCATGGCCATGC), d $(GA_4T_4C)_2$, and d $(GT_4A_4C)_2$, Hoechst 33342 and DMA showed a short decay component $\tau_1 = 2-2.4$ ns. TBZ showed a very short decay component $\tau 1$ at 0.7, 0.6, 0.7, and 0.9 ns with CTDNA, d ($CGCA_3T_3$-GCG), d (GA_5T_5C), and d $(GA_4T_4C)_2$, respectively. The complexes of TBZ with d (GCATGGCCATGC) and d $(GT_4A_4C)_2$ showed a short lifetime component of 2.3 and 2.8 ns, respectively. Hoechst 33342, DMA, and TBZ showed a long lifetime component at approximately 6.8, 6.2, and 5.6 ns with d (GCATGGCCATGC), respectively. A long lifetime component was not observed for the TBZ-d $(GT_4A_4C)_2$ complex at $R = 0.5$ (Table 2). These results indicate that two distinct complexes are formed between the ligands and the duplex oligonucleotides.

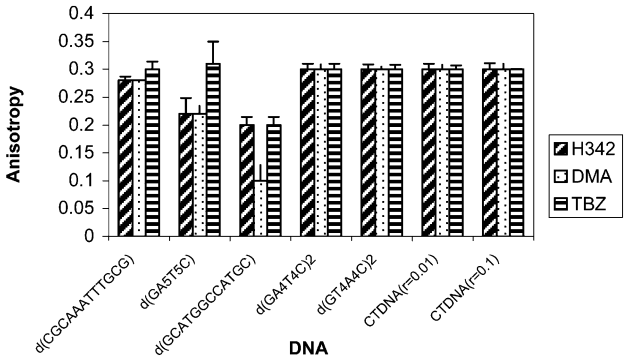

FIGURE 3: Graphical representation of anisotropy of Hoechst 33342, DMA, and TBZ to the CTDNA (100 μM) and d ($CGCA_3T_3GCG$), d (GA_5T_5C), d (GCATGGCCATGC), d $(GA_4T_4C)_2$, and d $(GT_4A_4C)_2$ duplexes (5 μM) in 2 mM sodium cacodylate buffer (pH = 7.2) containing 50 mM NaCl, 0.1 mM EDTA, and 12 mM $MgCl_2$ at 25 °C.

Table 2: Lifetime Measurements of the DNA−Ligand Complexes in 2 mM Sodium Cacodylate Buffer (pH = 7.2) Containing 50 mM NaCl, 0.1 mM EDTA, and 12 mM $MgCl_2$ at 25 °C

study system	$\tau 1$	$\tau 2$	χ^2
CTDNA + Hoechst 33342 ($R = 0.1$)	1.81 (39%)	4.15 (61%)	0.87
CTDNA + DMA ($R = 0.1$)	2.28 (44%)	4.19 (56%)	0.91
CTDNA + TBZ ($R = 0.1$)	0.67 (71%)	2.33 (29%)	0.9
d ($CGCA_3T_3GCG$) + Hoechst33342 ($R = 0.5$)	2.68 (100%)		0.763
d ($CGCA_3T_3GCG$) + DMA ($R = 0.5$)	2.74 (100%)		0.799
d ($CGCA_3T_3GCG$) + TBZ ($R = 0.5$)	0.62 (73%)	2.49 (27%)	0.768
d (GA_5T_5C) + Hoechst 33342 ($R = 0.5$)	2.35 (73%)	4.57 (27%)	0.818
d (GA_5T_5C) + DMA ($R = 0.5$)	2.18 (60%)	4.15 (40%)	0.89
d (GA_5T_5C) + TBZ ($R = 0.5$)	0.70 (80%)	2.60 (20%)	0.720
d (GCATGGCCATGC) + Hoechst 33342 ($R = 0.5$)	2.36 (75%)	6.83 (25%)	1.179
d (GCATGGCCATGC) + DMA ($R = 0.5$)	2.65 (55%)	6.16 (45%)	1.375
d (GCATGGCCATGC) + TBZ ($R = 0.5$)	2.25 (77%)	5.63 (23%)	1.254
d $(GA_4T_4C)_2$ + Hoechst 33342 ($R = 0.5$)	2.44 (81%)	4.08 (19%)	0.858
d $(GA_4T_4C)_2$ + DMA ($R = 0.5$)	2.64 (94%)	5.72 (6%)	0.868
d $(GA_4T_4C)_2$ + TBZ ($R = 0.5$)	0.85 (62%)	2.79 (38%)	0.896
d $(GT_4A_4C)_2$ + Hoechst 33342 ($R = 0.5$)	2.36 (84%)	4.39 (16%)	0.736
d $(GT_4A_4C)_2$ + DMA ($R = 0.5$)	2.26 (68%)	3.91 (32%)	0.832
d $(GT_4A_4C)_2$ +TBZ ($R = 0.5$)	2.77 (100%)		0.869

Equilibrium Binding Titrations. To further evaluate the AT and GC sequence discrimination for the three compounds, we determined their equilibrium binding constants upon binding with five duplex oligonucleotides (Figure 4). Absorbance changes for ligand−DNA complexes with increasing oligonucleotide concentrations were used to construct a half-reciprocal plot, $D/\Delta\epsilon_{ap} = D/\Delta\epsilon + 1/(\Delta\epsilon K)$ [inset, Figure 4]. The binding constants were taken from the ratio of the slope to the *y*-intercept. The high binding

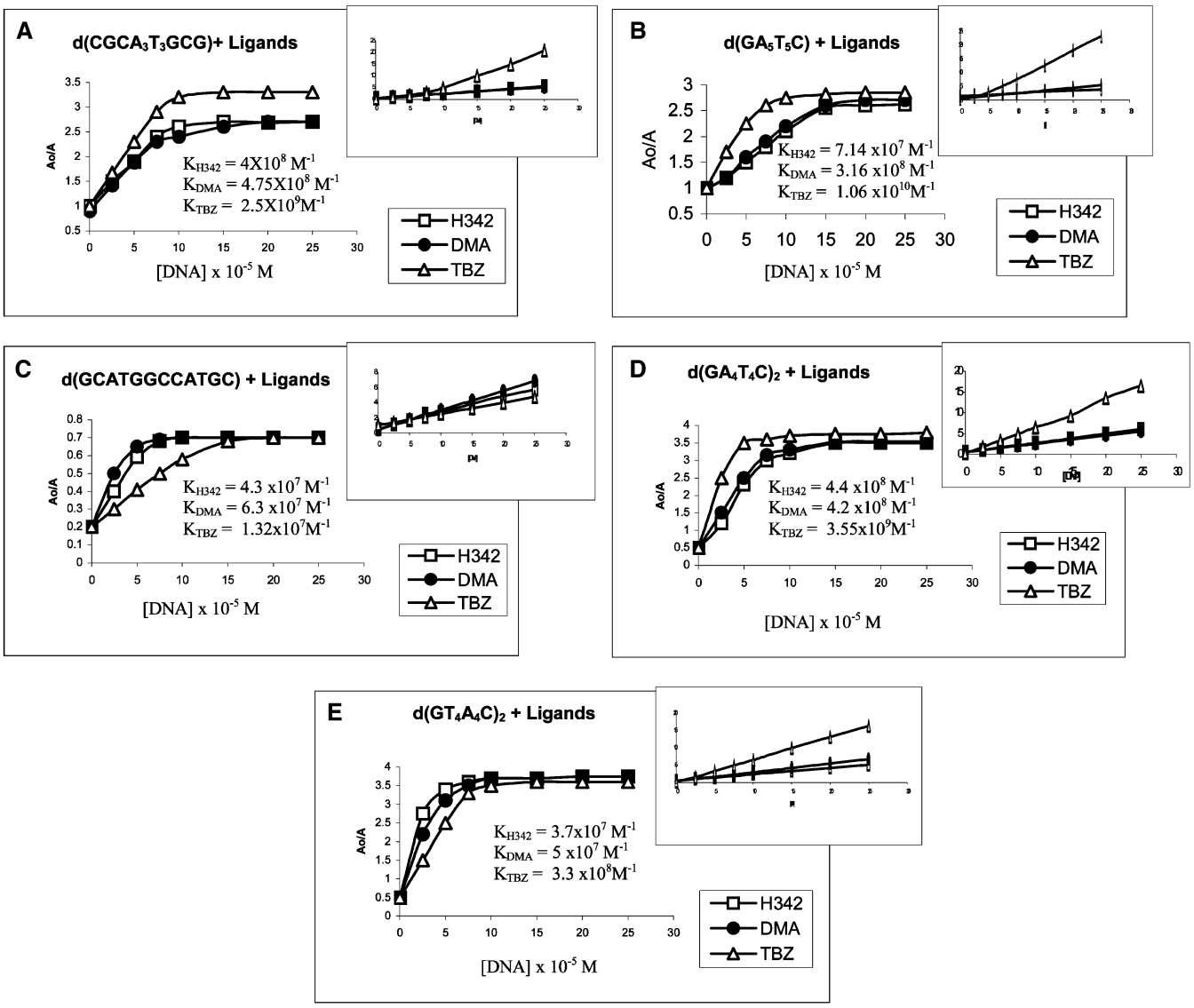

FIGURE 4: Equilibrium binding titrations. Saturation plot of absorption titration of Hoechst 33342, DMA, and TBZ with (A) d ($CGCA_3T_3$-GCG), (B) d (GA_5T_5C), (C) d (GCATGGCCATGC), (D) d $(GA_4T_4C)_2$, and (E) d $(GT_4A_4C)_2$ duplexes in 2 mM sodium cacodylate buffer (pH = 7.2) containing 50 mM NaCl, 0.1 mM EDTA, and 12 mM $MgCl_2$ at 25 °C. It was obtained by plotting A_o/A vs [DNA] where A_o denotes absorption intensity of the free ligand, and A is the observed absorption intensity for the ligand in the presence of the varying concentrations of oligonucleotides. Concentrations of DNA were expressed in base molarity. The inset shows the half-reciprocal plot of the absorption titrations. It was obtained by plotting $D/\Delta\epsilon$ ap vs D according to the equation as described.

constant for TBZ ($K = 1.06 \times 10^{10}$ M^{-1}) with AT-rich sequences with a 100-fold increase relative to GC-rich sequences ($K = 10^7$ M^{-1}) supports the findings obtained by the thermal denaturation studies (Figure 2) and provides further evidence for increased sequence selective binding by this ligand.

Gel Electrophoretic Mobility Assay. To assess changes in duplex DNA conformation with ligand binding, electrophoretic mobilities were assessed for the above-mentioned duplex oligonucleotides in the presence and absence of the three ligands. These results are illustrated in Figure 5. Hoechst 33342, DMA, and TBZ do not seem to alter the conformation of d (GCATGGCCATGC) and d $(GT_4A_4C)_2$. The highest mobility shift observed with the TBZ-d (GA_5T_5C) complex corroborates with the highest ΔT_m of 23 °C observed with this complex (Figure 5C). These observations suggest that TBZ preferentially binds structured regions of DNA and induces a further conformational change that slows the complex migration in a polyacrylamide gel.

DISCUSSION

This study introduces DMA and TBZ, derivatives of Hoechst 33342, and presents characterization of their DNA binding properties relative to the parent compound. The derivatives contain additional groups, which were introduced with the objective of increasing the H bonding capacity of the ligand and expanding its recognition face for the minor groove within the duplex DNA.

Earlier studies with stopped flow kinetics and fluorescence titrations of phenyl bisubstituted Hoechst 33258 analogues have been reported (*20*), where a higher binding constant ($K_a = 1.9 \times 10^{10}$ M^{-1}) has been reported for the interaction of a 28mer DNA hairpin with bis *m*-OH-Hoechst, which is due to the presence of two hydroxyl groups capable of hydrogen bonding as compared to two methoxy groups in DMA. Using footprinting experiments, Leupin's group has reported that the trisbenzimidazole molecule with a *N*-methyl piperazine ring binds to five to six base pairs (*19*),

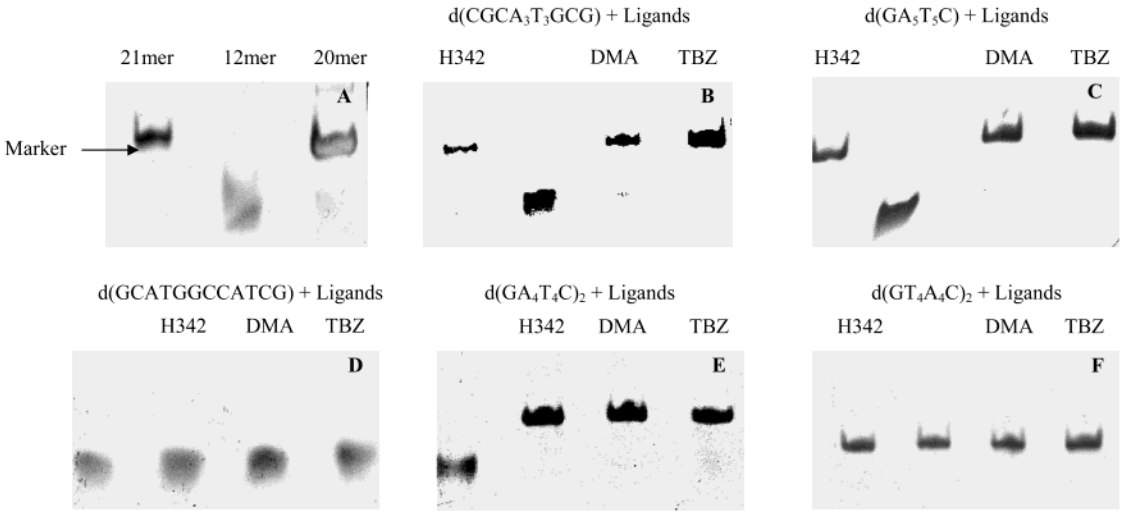

FIGURE 5: Electrophoretic mobility shift assay. Nondenaturing 25% polyacrylamide gels were run in 0.75-1X TBE at 12 V/cm at 25 °C. (A) Electrophoretic mobility of d ($CGCA_3T_3GCG$) (lane 2) and d $(GA_4T_4C)_2$ (lane 3 is compared with a 21mer marker (lane 1)). (B) Reduced electrophoretic mobility of DNA−ligand complexes ($R = 0.5$) (lanes 1, 3, and 4) with d ($CGCA_3T_3GCG$) (100 μM) (lane 2). (C) Highest mobility shift is shown by the TBZ-d (GA_5T_5C) complex (lane 4) followed by the Hoechst33342-d (GA_5T_5C) and DMA-d (GA_5T_5C) complexes (lanes 1 and 3, respectively) as compared to d (GA_5T_5C) (lane 2). (D) Mobility shift is not observed in d (GCATGGCCATGC) (100 μM) (lane 1) and DNA−ligand complexes ($R = 0.5$) (lanes 2−4). (E) d $(GA_4T_4C)_2$−ligand complexes ($R = 0.5$) (lanes 2−4) show retarded electrophoretic mobility as compared to d $(GA_4T_4C)_2$ (100 μM) (lane 1), whereas d $(GT_4A_4C)_2$−ligand complexes ($R = 0.5$) (lanes 1, 3, and 4) show no difference in mobility as compared to d $(GT_4A_4C)_2$ (100 μM) (lane 2) in panel F.

whereas for the first time the present studies show the binding of TBZ to 8−10 base pairs using absorption and emission spectroscopy, thermal denaturation, and EMSA studies.

AT-Rich Sequence Selectivity. DMA and TBZ show AT selectivity like the parent molecule Hoechst 33342, which is supported by several lines of experimental evidences. First, UV, fluorescence, and T_m measurements using d ($CGCA_3T_3GCG$) (*21*) and d (GCATGGCCATGC) show that DMA and TBZ preferentially bind to an AT-rich sequence similar to Hoechst 33342. However, TBZ showed higher affinity for longer AT sequences as evident from $\Delta T_m = 21$ °C for d ($CGCA_3T_3GCG$) and $K = 2.5 \times 10^9$ M^{-1} (Figure 4A) and also seems to bind in a slightly different orientation ($r = 0.3$). Lifetime measurements also support AT selectivity, suggesting that all three ligands are able to discriminate between AT and GC base pairs (Table 2). It appears that certain interactions with the methyl piperazine ring present in all three structures makes them GC tolerant (*22*). Finally, the EMSA data also support AT-rich sequence selectivity (Figure 5B,D). Therefore, it is clear that both DMA and TBZ have an AT-rich sequence selectivity similar to the parent compound Hoechst 33342 and suggests that neither the addition of two methoxy groups in DMA nor the addition of a hydroxyl and a methoxy group in TBZ compromise the sequence selectivity.

The introduction of one more benzimidazole unit in TBZ was based on the molecular modeling studies (*10*) with the purpose of increasing sequence specificity of the ligand and also to improve the affinity for a longer AT-rich tract of DNA (*19*). Indeed, the spectroscopic studies with d ($CGCA_3T_3GCG$) and d (GA_5T_5C) indicate that TBZ has a higher affinity for longer AT-rich tracts, with enhanced specificity for longer AT stretches (Table 1). While the emission spectra of ligands did not show a significant difference with either sequence, anisotropy measurements have clearly differentiated the kind of interaction that prevails between complexes of TBZ with d ($CGCA_3T_3GCG$) and d (GA_5T_5C) ($r = 0.31$) (Figure 3). These results suggest that the binding orientation of TBZ with respect to the DNA helical axis is distinct with both sequences since d ($CGCA_3T_3GCG$) provides 6 base pairs for its binding, and d (GA_5T_5C) provides 10 base pairs for complete and strong binding of the ligand to the duplex. The ΔT_m of TBZ with d ($CGCA_3T_3GCG$) is 6 °C higher than Hoechst 33342 and DMA, but with d (GA_5T_5C), ΔT_m has increased to 13 °C (Figure 2). Higher values of ΔT_m observed with TBZ-d ($CGCA_3T_3GCG$) and d (GA_5T_5C) as compared to Hoechst 33342 and DMA with the intrinsic binding constant [$K = 2.5 \times 10^9$ M^{-1} for d ($CGCA_3T_3GCG$) and $K = 1.06 \times 10^{10}$ M^{-1} for d (GA_5T_5C)] strongly suggest that TBZ binds more strongly to d (GA_5T_5C) than d ($CGCA_3T_3GCG$). Therefore, the additional ring within the structure provides an expanded recognition face for ds DNA (*19*). The TBZ−DNA complex has shown the highest retarded electrophoretic mobility due to the high degree of stabilization of the duplex as compared to the DMA−DNA and Hoechst 33342−DNA complexes (Figure 5B,C). Results of the mobility shift studies have further confirmed the effects of binding of these ligands on the global conformation of the sequences and thus lend further support to the sequence specificity of these ligands.

Complex Formation and Heterogeneity. Fluorescence lifetime measurements provide an insight into the molecular species that exist in the excited state of the ligand and the ligand−DNA complexes, and the type of molecular species that exists in the excited state basically depends on the DNA sequence to which the molecule is bound. Therefore, investigations on excited-state species facilitates the understanding of the binding behavior of the ligands with the target molecule. It is interesting to note that the lifetimes of both short lifetime components ($\tau_1 \approx 2$ ns) and long lifetime components ($\tau_2 \approx 4$ ns) for Hoechst 33342 and DMA were significantly higher than the corresponding values for TBZ ($\tau_1 \approx 0.7$ ns and $\tau_2 \approx 2.6$ ns) (Table 2). The complex of d

($CGCA_3T_3GCG$) with Hoechst 33342 and DMA indicates a homogeneity of the molecular species in the excited state, whereas TBZ shows a heterogeneity in the system. The heterogeneity of the lifetime can be interpreted such that the ligands Hoechst 33342 and DMA occupy a stretch of four base pairs (AATT); thereby, the remaining stretch of base pairs attain a particular conformation that is common to both these ligands. TBZ being a longer molecule occupies the full stretch of AT base pairs; thus, the duplex attains a different conformation that is specific for TBZ and is evident from the double-exponential decay of the complex. The decay characteristics of d (GCATGGCCATCG)−ligand complexes are characterized by double-exponential decay ($\tau 1 \approx 2.3$ ns and $\tau 2 \approx 6$ ns). Thus, for all three ligands, two distinct molecular interactions are suggested for the ligand/DNA complex.

With d ($CGCA_3T_3GCG$), Hoechst 33342 and DMA showed a single-exponential decay, whereas with d (GA_5T_5C), both these ligands showed double-exponential decay (Table 2). The heterogeneity of the molecular species in these ligand−DNA complexes can be attributed to uncovered base pairs that attain a different conformation in d (GA_5T_5C) due to differences in the AT content. TBZ showed a double-exponential decay with both the sequences since it covers all the AT base pairs in d ($CGCA_3T_3GCG$) and 10 base pairs in d (GA_5T_5C) with the reduced probability of attaining a different conformation in two cases. However, the existence of two different molecular species in the case of TBZ appears to be very high, which contributes to the decay profile of the TBZ−DNA complexes.

DNA Structure Selective Binding and Alteration of the Complex. Certain AT-rich sequences show striking conformational alterations, often referred to as bent DNA (*23*). Therefore, AT-rich sequence selectivity and bent DNA structure selectivity are related issues. Further, conformationally distinct sequences with the same overall base composition have been described (*24*). For example, the decameric DNA duplexes d $(GA_4T_4C)_2$ and d $(GT_4A_4C)_2$ exhibit differential thermodynamic and electrophoretic properties (*23*−*28*). The d $(GA_4T_4C)_2$ duplex has a bent conformation (*29*−*33*), while d $(GT_4A_4C)_2$ has a normal conformation (*25*). Alternatively, it has been suggested that the d $(GA_4T_4C)_2$ duplex adopts a poly d (A)•d (T)-like structure, while the d $(GT_4A_4C)_2$ assumes a more normal B-like conformation (*31*). Fluorescence spectroscopic analysis showed that the three ligands bind d $(GA_4T_4C)_2$ similarly, but binding to d $(GT_4A_4C)_2$ was distinct, with TBZ showing a single broad peak at 491 nm (Table 1). The extent of ligand-induced duplex thermal stability (ΔT_m) was greater for d $(GA_4T_4C)_2$ with all three ligands, and TBZ showed higher duplex stabilization for d $(GA_4T_4C)_2$ ($\Delta T_m = 19$ °C) over d $(GT_4A_4C)_2$ ($\Delta T_m = 12$ °C) (Figure 2). Thus, as measured by differences in T_m, TBZ was able to better distinguish between a duplex with an A_4T_4 central core.

The basic spectroscopy data, however, do not allow us to assess whether the differential affinity of these ligands results from an intrinsic sequence preference for an A_4T_4 versus a T_4A_4 binding site or if the drug is selective for a difference in the overall duplex structure/hydration (e.g., A-tract/highly hydrated DNA or bent versus normal DNA). To determine the extent of binding of these ligands, the intrinsic binding constant was being calculated. These calculations with d $(GA_4T_4C)_2$ revealed that the intrinsic biding constant (K) was 4×10^8 M^{-1} for Hoechst 33342 and DMA, while it was nearly 10-fold higher for TBZ ($K = 3.55 \times 10^9$ M^{-1}). Interestingly, however, the intrinsic binding constant was 3.3×10^8 M^{-1} with d $(GT_4A_4C)_2$ (Figure 4D,E). The EMSA (Figure 5E,F) clearly suggested that these ligands are able to recognize the difference in DNA structure. It appears that TBZ binds with d $(GA_4T_4C)_2$, a bent molecule, and alters the confirmation completely, whereas with the d $(GT_4A_4C)_2$-normal B-like DNA molecule, there is no structural alteration. However, the mobility shift observed is much more than that reported at the same ligand/DNA ratio (*34*). Therefore, TBZ appears to selectively bind the structured sequence.

In conclusion, the results presented that two analogues (DMA and TBZ), structural modifications of Hoechst 33342 with improved DNA binding and specificity and structural differentiation properties, bind double-stranded DNA similar to the parent compound but show striking fluorescence enhancement upon binding to the DNA duplex. Further, TBZ has an expanded double-stranded DNA recognition face that spans 8−10 base pairs and binds in a noncooperative manner with d (GCATGGCCATGC) and d $(GT_4A_4C)_2$, whereas it binds specifically to d $(GA_4T_4C)_2$ as with d ($CGCA_3T_3GCG$) and d (GA_5T_5C). The basic properties of these molecules make them potential probes for gene regulation and nucleosome remodeling studies.

REFERENCES

1. Eriksson, S., Seog K. K., Kubista, M., and Norden, B. (1993) Binding of 4,6′-Diamidino-2-phenylindole (DAPI) to AT regions of DNA: Evidence for an allosteric conformational change, *Biochemistry* 32, 2987−2998.
2. Kubista, M., Akerman, B., and Norden, B. (1987) Characterization of an interaction between DNA and 4,6′-diamidino-2-phenylindole by optical spectroscopy, *Biochemistry 26*, 4545−4553.
3. Turner, P. R., and Denny, W. A. (1996) The mutagenic properties of DNA minor-groove binding ligands, *Mutation Res. 355*, 141−169.
4. Teng, M.-K., Usman, N., Frederick, C. A., and Wang, A. H.-J. (1988) The molecular structure of the complex of Hoechst 33258 and the DNA dodecamer d (CGCGAATTCGCG), *Nucleic Acids Res. 16*, 2671−2690.
5. Hertzberg, R. P., and Dervan P. B. (1984) Cleavage of DNA with methidiumpropyl-EDTA-iron(II): reaction conditions and product analyses, *Biochemistry 23*, 3934−3945.
6. Martin, R. F., Pardee, M., Kelly, D. P., and Mack, P. O.-L. (1986) DNA binding compounds V. Synthesis and characterization of Boron-containing bibenzimidazoles related to the DNA minor groove binder, Hoechst 33258, *Aust. J. Chem. 39*, 373−381.
7. Vega, M. C., Saez, I. G., Aymani, J., Eritja, R., Van der Marel, G. A., Van Boom, J. H., Rich, A., and Coll, M. (1994) Three-dimensional crystal structure of the A-tract DNA dodecamer d ($CGCA_3T_3GCG$) complexed with the minor-groove-binding drug Hoechst 33258, *Eur J. Biochem. 222*, 721−726.
8. Gavathiotis, E., Sharman, G. J., and Searle, M. S. (2000) Sequence dependent variation in DNA minor groove width dictates orientational preference of Hoechst 33258 in A-tract recognition, solution NMR structure of the 2:1 complex with d (CTTTTG-$CAAAAG)_2$, *Nucleic Acids Res. 28*, 728−735.
9. Sadat, E. S. E., Amanda, W. N., and Douglas, K. T. (1997) Unique binding site for bisbenzimidazoles on transfer RNA, *Chem. Commun. 4*, 385−386.
10. Mekapati, S. B., and Hansch, C. (2001) Comparative QSAR studies on bibenzimidazoles and terbenzimidazoles inhibiting topoisomerase I, *Bioorg. Med. Chem. 9*, 2885−2893.
11. Tawar, U., Jain, A. K., Dwarakanath, B. S., Chandra, R., Singh, Y., Khaitan, D., and Tandon, V. (2003) Influence of bisubstituion on the cytotoxicity of bisbenzimidazoles and trisbenzimidazoles:

Synthesis and biological evaluation as radioprotectors, *J. Med. Chem. 46*, 3785−3792.
12. Nagaich, A. K. Bhattacharya, D., Brahmachari, S. K., and Bansal, M. (1994) CA/TG sequence at the 5′ end of oligo A-tracts strongly modulates DNA curvature, *J. Biol. Chem. 269*, 7824−7833.
13. Benesi, H. A., and Hildebrand, J. H. (1949) A spectrophotometric investigation of the interaction of iodine with aromatic hydrocarbons, *J. Am. Chem. Soc. 71*, 2703−2707.
14. Schemechel, D. E. V., and Crothers, D. M. (1971) Kinetic and hydrodynamics studies of the complex of proflavine with poly A•poly U, *Biopolymers 10*, 465−480.
15. Meehan, T., Gamper, H., and Becker, J. F. (1982) Characterization of reversible, physical binding of benzo[α]pyrene derivatives to DNA, *J. Biol. Chem. 257*, 10479−10485.
16. Bhattacharya, S., and Mandal, S. S. (1997) Interaction of surfactants with DNA. Role of hydrophobicity and surface charge on intercalation and DNA melting, *Biochim. Biophys. Acta 1323*, 29−44.
17. Kumar, C. V., and Asuncion, E. H. (1993) DNA binding studies and site selective fluorescence sensitization of an anthryl probe, *J. Am. Chem. Soc. 115*, 8547−8553.
18. Kumar, C. V., and Asuncion, E. H. (1992) Sequence dependent energy transfer from DNA to a simple aromatic chromophore, *J. Chem. Soc., Chem. Commun.* 470−472.
19. Ji, Y.-H., Bur, D., Hasler, W., Schmitt, V. R., Dorn, A., Bailly, C., Waring, M. J., Hochstrasser, R., and Leupin, W. (2001) Trisbenzimidazole derivatives: design, synthesis, and DNA sequence recognition, *Bioorg. Med. Chem. 9*, 2905−2919.
20. Breusegem, S. Y., Ebrahimi, S. E. S., Douglas, K. T., Clegg, R. M., and Loontiens, F. G. (2001) Increased stability and lifetime of the complex formed between DNA and meta-phenyl substituted Hoechst dyes as studied by fluorescence titrations and stopped-flow kinetics, *J. Mol. Biol. 308*, 649−663.
21. Tabernaro, L., Verdaguer, N., Coll, M., Fita, I., van der Marel, G. A., van Boom, J. H., Rich, A., and Aymani, J. (1993) Molecular structure of the A-tract DNA dodecamer d ($CGCA_3T_3GCG$) complexed with the minor groove binding drug netropsin, *Biochemistry 32*, 8403−8410.
22. Wang, H., Gupta, R., and Lown J. W. (1994) Synthesis, DNA binding, sequence preference, and biological evaluation of minor groove selective N1 alkoxyalkyl-bis-benzimidazoles, *Anticancer Drug Des. 9*, 145−157.
23. Koo, H.-S., and Crothers, D. M. (1988) Calibration of DNA curvature and a unified description of sequence-directed bending, *Proc. Natl. Acad. Sci. U.S.A. 85*, 1763−1767.
24. Balagurumoorthy, P., and Brahmachari, S. K. (1994) Structure and stability of human telomeric sequence, *J. Biol. Chem. 269*(*34*), 21858−21869.
25. Pierce, M. A., and Tullius, T. D. (1993) How the structure of adenine tract depends on sequence context: A new model for the structure of T_nA_n DNA sequences, *Biochemistry 32*, 127−136.
26. Arthanari, H., Basu, S., Kawano, T. L., and Bolton, P. H. (1998) Fluorescent dyes specific for quadruplex DNA, *Nucleic Acids Res. 26*, 3724−3728.
27. Diekmann, S., and Wang, J. C. (1985) On the sequence determinants and flexibility of the kinetoplast DNA fragment with abnormal gel electrophoretic mobilities, *J. Mol. Biol. 186*, 1−11.
28. Wu, H.-M., and Crothers, D. M. (1984) The locus of sequence-directed and protein-induced DNA bending, *Nature 308*(*5*), 509−513.
29. Sprous, D., Zacharias, W., Wood, Z. A., and Harvey, S. C. (1995) Dehydrating agents sharply reduce curvature in DNAs containing A-tracts, *Nucleic Acids Res. 23*, 1816−1821.
30. Caneva, R., De Simoni, A., Mayol, L., Rossetti, L., and Savino, M. (1997) Different bindings of the minor groove ligands DAPI and Hoechst 33258 to multimers of the curved (CA_4T_4G) and noncurved (CT_4A_4G) DNA sequences, *Biochim. Biophys. Acta 1353*, 93−97.
31. Burkhoff, A. M., and Tullius, T. D. (1988) Structural details of an adenine tract that does not cause DNA to bend, *Nature 331*, 455−457.
32. Travers, A. A. (1989) DNA conformation and protein binding, *Annu. Rev. Biochem. 58*, 427−452.
33. Hagerman, P. J. (1990**)** Sequence-directed curvature of DNA, *Annu. Rev. Biochem. 59*, 755−781.
34. Pilch, D. S., Xu, Z., Sun, Q., La Voie, E. J., Liu, L. F., and Breslauer, K. J. (1997) A terbenzimidazole that preferentially binds and conformationally alters structurally distinct DNA duplex domains: A potential mechanism for topoisomerase I poisoning, *Proc. Natl. Acad. Sci. U.S.A. 94*, 13565−1357.

BI034425K